HAL
open science

Searches for HCl and HF in comets 103P/Hartley 2 and C/2009 P1 (Garradd) with the Herschel Space Observatory

D. Bockelée-Morvan, N. Biver, J. Crovisier, D. Lis, P. Hartogh, R. Moreno, M. de Val-Borro, G. Blake, S. Szutowicz, J. Boissier, et al.

To cite this version:

D. Bockelée-Morvan, N. Biver, J. Crovisier, D. Lis, P. Hartogh, et al.. Searches for HCl and HF in comets 103P/Hartley 2 and C/2009 P1 (Garradd) with the Herschel Space Observatory. Astronomy and Astrophysics - A&A, 2014, 562, pp.A5. 10.1051/0004-6361/201322939 . hal-02611730

HAL Id: hal-02611730

https://hal.science/hal-02611730v1

Submitted on 25 Oct 2023

HAL is a multi-disciplinary open access archive for the deposit and dissemination of scientific research documents, whether they are published or not. The documents may come from teaching and research institutions in France or abroad, or from public or private research centers.

L'archive ouverte pluridisciplinaire **HAL**, est destinée au dépôt et à la diffusion de documents scientifiques de niveau recherche, publiés ou non, émanant des établissements d'enseignement et de recherche français ou étrangers, des laboratoires publics ou privés.

Astronomy & Astrophysics manuscript no. Bockelee-halogens-resubmitted-2columns
August 2, 2021
© ESO 2021

arXiv:1401.1104v2 [astro-ph.EP] 7 Jan 2014

Searches for HCl and HF in comets 103P/Hartley 2 and C/2009 P1 (Garradd) with the *Herschel* space observatory*

D. Bockelée-Morvan[1], N. Biver[1], J. Crovisier[1], D.C. Lis[2], P. Hartogh[3], R. Moreno[1], M. de Val-Borro[4], G.A. Blake[2], S. Szutowicz[5], J. Boissier[6], J. Cernicharo[7], S.B. Charnley[8], M. Combi[9], M.A. Cordiner[8], T. de Graauw[10], P. Encrenaz[11], C. Jarchow[3], M. Kidger[12], M. Küppers[12], S.N. Milam[8], H.S.P. Müller[13], T.G. Phillips[2], and M. Rengel[3]

[1] LESIA, Observatoire de Paris, CNRS, UPMC, Université Paris-Diderot, 5 place Jules Janssen, 92195 Meudon, France
e-mail: dominique.bockelee@obspm.fr
[2] California Institute of Technology, Pasadena, 301-17, Pasadena, CA 91125, USA
[3] Max-Planck-Institut für Sonnensystemforschung, Max-Planck-Str. 2, 37191 Katlenburg-Lindau, Germany
[4] Department of Astrophysical Sciences, Princeton University, Princeton, NJ 08544, USA
[5] Space Research Centre, Polish Academy of Science, Bartycka 18a, 00-716, Warszawa, Poland
[6] Institut de Radioastronomie Millimétrique, 300 rue de la Piscine, Domaine Universitaire, 38406, Saint Martin d'Hères, France
[7] Department of Astrophysics, CAB, INTA-CSIC, Crta Torrejón-Ajalvir km 4, E-28850 Torrejón de Ardoz, Madrid, Spain
[8] NASA Goddard Space Flight Center, Greenbelt, MD 20770, USA
[9] Department of Atmospheric, Oceanic and Space Sciences, University of Michigan, 2455 Hayward Street, Ann Arbor, MI 48109-2143, USA
[10] ALMA Observatory, Alonso de Córdova 3107, Vitacura, Santiago, Chile
[11] LERMA, Observatoire de Paris, CNRS, UPMC, 61 avenue de l'observatoire, F-75014, Paris, France
[12] European Space Astronomy, ESAC, P.O. Box 78, 28691 Villanueva de la Cañada, Spain
[13] I. Physikalisches Institut, Universität zu Köln, Zülpicher Str. 77, 50937 Köln, Germany

Received

ABSTRACT

Context. HCl and HF are expected to be the main reservoirs of fluorine and chlorine over a wide range of conditions, wherever hydrogen is predominantly molecular. They are found to be strongly depleted in dense molecular clouds, suggesting freeze-out onto grains in such cold environments. We can then expect that HCl and HF were also the major carriers of Cl and F in the gas and icy phases of the outer solar nebula, and were incorporated into comets.
Aims. We aimed to measure the HCl and HF abundances in cometary ices as they can provide insights on the halogen chemistry in the early solar nebula.
Methods. We searched for the $J(1\text{–}0)$ lines of HCl and HF at 626 and 1232 GHz, respectively, using the Heterodyne Instrument for the Far-Infrared (HIFI) on board the *Herschel* Space Observatory. HCl was searched for in comets 103P/Hartley 2 and C/2009 P1 (Garradd), whereas observations of HF were conducted in comet C/2009 P1 (Garradd). In addition, observations of H_2O and $H_2{}^{18}O$ lines were performed in C/2009 P1 (Garradd) to measure the H_2O production rate at the time of the HCl and HF observations. Three lines of CH_3OH were serendipitously observed in the HCl receiver setting.
Results. HCl is not detected, whereas a marginal (3.6-σ) detection of HF is obtained. The upper limits for the HCl abundance relative to water are 0.011 % and 0.022 %, for comet 103P/Hartley 2 and C/2009 P1 (Garradd), respectively, showing that HCl is depleted with respect to the solar Cl/O abundance by a factor more than 6^{+6}_{-3} in 103P/Hartley 2, where the error is related to the uncertainty in the chlorine solar abundance. The marginal HF detection obtained in C/2009 P1 (Garradd) corresponds to an HF abundance relative to water of $(1.8\pm0.5) \times 10^{-4}$, which is approximately consistent with a solar photospheric F/O abundance. The inferred water production rate in comet C/2009 P1 (Garradd) is $(1.1\pm0.3) \times 10^{29}$ s^{-1} and $(0.75\pm0.05) \times 10^{29}$ s^{-1} on 17 and 23 February 2012, respectively. CH_3OH abundances relative to water are 2.7±0.3 % and 3.4 ± 0.6%, for comets 103P/Hartley 2 and C/2009 P1 (Garradd), respectively.
Conclusions. The observed depletion of HCl suggests that HCl was not the main reservoir of chlorine in the regions of the solar nebula where these comets formed. HF was possibly the main fluorine compound in the gas phase of the outer solar nebula. However, this needs to be confirmed by future measurements.

Key words. Comets: general; Comets: individual: C/2009P1 (Garradd), 103P/Hartley 2; Submillimeter: planetary systems

1. Introduction

Chlorine and fluorine are two of the few atoms that can react exothermically (Cl^+, F) or with a small energy bar-

* *Herschel* is an ESA space observatory with science instruments provided by European-led Principal Investigator consortia and with important contribution from NASA.

rier (Cl) with H_2, the dominant component of interstellar clouds and protoplanetary disks, producing hydrogen chloride (HCl) and hydrogen fluoride (HF), respectively, directly (Cl, F) or eventually (Cl^+). Hence, based on theoretical models of interstellar chemistry, HCl and HF are expected to be the main reservoirs of chlorine and fluorine over a wide range of conditions, wherever hydrogen is predominantly molecular (e.g., Neufeld & Wolfire, 2009).

HF and HCl have both been detected in diffuse and dense molecular clouds. Relative abundances measured in diffuse clouds show that, indeed, fluorine is essentially locked in HF (e.g., Neufeld et al., 2010; Monje et al., 2011), whereas HCl accounts for less than 1% of the elemental chlorine due to a rich chemistry initiated by ionizing radiation (e.g., Monje et al., 2013). In dense molecular clouds, HF and HCl are found to be strongly depleted, which is thought to be the result of nearly all HF and HCl molecules freezing out onto grains in such cold environments (Peng et al., 2010; Emprechtinger et al., 2012). Both HCl and HF have relatively high freezing points (sublimation temperatures of 51 K and 70 K, respectively), so they establish strong bonds onto grains. We can then expect that HCl and HF were the major carriers of Cl and F in the gas and icy phases of the solar nebula, and were subsequently incorporated into comets.

The lowest rotational transitions of HCl and HF lie in the submillimetre domain and either cannot be (HF), or can only be with difficulty (HCl) (e.g., Schilke et al., 1995), observed from the ground because of severe atmospheric absorption. Hence, most detections in astrophysical sources were obtained after 2009 from observations using the *Herschel* Space Observatory (Pilbratt et al., 2010). *Herschel* also offered a rare opportunity to search for these species in comets. The solar abundances of Cl and F relative to atomic oxygen are, respectively, $(Cl/O)_\odot \sim 6.5 \times 10^{-4}$ and $(F/O)_\odot \sim 7.4 \times 10^{-5}$ (Asplund et al., 2009), so that sensitive searches required the apparitions of bright comets during the lifetime of *Herschel*.

We present observations of the $H^{35}Cl$ and $H^{37}Cl$ J(1–0) lines near 625–626 GHz in comets 103P/Hartley 2 and C/2009 P1 (Garradd) performed with HIFI (de Graauw et al., 2010). A sensitive search of HF J(1–0) at 1232 GHz conducted in C/2009 P1 (Garradd) was also performed. This paper also presents HIFI observations of several rotational lines of water undertaken in February 2012, at the time of the halogen observations in comet C/2009 P1 (Garradd), which complement those performed in October 2011 (Bockelée-Morvan et al., 2012). Methanol (CH_3OH) lines observed with the HCl receiver setting are also presented.

Comet 103P/Hartley 2 is a short-period comet belonging to the Jupiter family, which made a close approach to Earth in October 2010, and was the object of a worldwide observational campaign in support to the EPOXI mission (A'Hearn et al., 2011; Meech et al., 2011). Comet C/2009 P1 (Garradd) is, in contrast, a long-period comet coming from the Oort cloud, which presented significant activity at its perihelion in December 2011. Both comets were the subjects of deep investigations using *Herschel*, including measurements of the D/H ratio in water (Hartogh et al., 2011; Bockelée-Morvan et al., 2012). The observations of 103P/Hartley 2 presented here were executed in the framework of the guaranteed time key programme "Water and related chemistry in the Solar System" (Hartogh et al., 2009). Those of C/2009 P1 (Garradd) correspond to an open time proposal.

The HCl lines were not detected, whereas a marginal detection of HF was obtained. We present the observations in Sect. 2, and their analysis in Sect. 3. A discussion follows in Sect. 4.

2. Observations

The observations were performed using the HIFI instrument onboard the *Herschel* Space Observatory, a 3.5-m telescope of the European Space Agency. The observing log is presented in Table 1.

$H^{35}Cl$ and $H^{37}Cl$ were searched for in comet 103P/Hartley 2 on 30 October 2010 UT, i.e., near the time of its closest approach to Earth (20 October 2010), and perihelion (28 October 2010). The heliocentric distance at the time of the observations was $r_h \sim 1.06$ AU, and the distance from *Herschel* was $\Delta = 0.13$ AU at the time of the observations. HF and HCl observations in comet C/2009 P1 (Garradd) were conducted on 17 and 22–23 February 2012 UT ($r_h \sim 1.76$ AU, $\Delta \sim 1.31$ AU, Table 1), respectively, i.e., about two months after its perihelion on 23 December 2011 at perihelion distance $q = 1.55$ AU. Solar elongation constraints prevented us from scheduling *Herschel* observations of comet Garradd at perihelion. For comet C/2009 P1 (Garradd), the integration time was long (6–7 h for both HCl and HF). The integration time was less than 1 h for HCl in comet 103P/Hartley 2 (Table 1).

The $H^{35}Cl$ and $H^{37}Cl$ J(1–0) lines, at 625.9153 and 624.9751 GHz[1], respectively (De Lucia et al., 1971), were observed simultaneously, in the upper sideband of band 1b HIFI receiver. The $I = 3/2$ nuclear spin of ^{35}Cl and ^{37}Cl splits the J(1–0) line into three $\Delta F_1 = 0, -1, +1$ hyperfine components (Cazzoli & Puzzarini, 2004) with statistical-weight ratio 2:3:1, with the main component F_1(5/2–3/2) being at the rest frequencies of 625.9188 GHz and 624.9778 GHz for $H^{35}Cl$ and $H^{37}Cl$, respectively. The outer two components are separated by –6.35 and +8.22 km s^{-1}, respectively, from the strongest middle component for $H^{35}Cl$, and by –5.05 km s^{-1} and +6.45 km s^{-1}, respectively, for $H^{37}Cl$. This splitting has been resolved in astronomical observations (e.g., Peng et al., 2010). The much smaller splitting caused by the $I = 1/2$ spin of the H nucleus can be resolved in the laboratory (Kaiser, 1970; Cazzoli & Puzzarini, 2004), but not in astronomical observations.

The HF J(1–0) line at 1232.4762 GHz (Nolt et al., 1987) was observed in the upper side band of the band 5a receiver.

The 1_{11}–0_{00} para lines of H_2O and $H_2{}^{18}O$ at 1113.3430 (Yu et al., 2012) and 1101.6983 GHz (De Lucia et al., 1972; Johns, 1985), respectively, as well as the 2_{11}–2_{02} para H_2O line (752.0331 GHz, Pearson, 1995), were observed at the dates of the HCl and HF observations of comet C/2009 P1 (Garradd) (Table 1). Except for the observations conducted on 17 February, a long integration time was requested for these observations to possibly detect lines of H_2O^+. These H_2O^+ observations are not further discussed in the present paper.

Spectra were acquired with both the Wide Band Spectrometer (WBS) and High Resolution Spectrometer (HRS). The spectral resolution of the WBS is 1.1 MHz.

[1] All rest frequencies in this paper were taken from the JPL catalog http://spec.jpl.nasa.gov/ (Pickett et al., 1998).

Table 1. Log of the observations.

Comet	Date (UT) yyyy/mm/dd.ddd	r_h (AU)	Δ^a (AU)	Species/line	ObsId 13422#	HIFI band	Mode	Int. time (min)
103P/Hartley 2	2010/10/30.626–30.662	1.059	0.131	$H^{35}Cl$, $H^{37}Cl$ $J(1–0)^b$	08589	1b	Point	52
C/2009P1 (Garradd)	2012/02/17.053–17.369	1.727	1.356	HF $J(1–0)$	39306/07	5a	Point	453
C/2009P1 (Garradd)	2012/02/17.393–17.417	1.727	1.356	H_2O $1_{11}–0_{00}$	39309	4b	Mapping	34
C/2009P1 (Garradd)	2012/02/22.745–23.004	1.762	1.308	$H^{35}Cl$, $H^{37}Cl$ $J(1–0)^b$	40372/73	1b	Point	372
C/2009P1 (Garradd)	2012/02/23.009–23.196	1.763	1.306	H_2O $2_{11}–2_{02}$	40375	2b	Point	269
C/2009P1 (Garradd)	2012/02/23.202–23.448	1.764	1.305	H_2O, $H_2{}^{18}O$ $1_{11}–0_{00}$	40377	4b	Point	353

Notes. [a] Distance from *Herschel*. [b] also includes the $3_2 - 2_1$ A^-, $13_{-1} - 12_{-1}$ E, and $13_0 - 12_0$ E lines of CH_3OH.

Table 2. Line areas and production rates.

Date (UT)[a] yyyy/mm/dd.ddd	Species	Line	ν (GHz)	Beam size ($''$)	Line area[b] (mK km s^{-1})	Production rate[c] (s^{-1})
103P/Hartley 2						
2010/10/30.644	$H^{35}Cl$	$J(1–0)$	625.9188[d]	34	<19[e]	$< 1.1 \times 10^{24}$
2010/10/30.644	$H^{37}Cl$	$J(1–0)$	624.9778[d]	34	<18[e]	$< 1.0 \times 10^{24}$
2010/10/30.644	CH_3OH	$3_2 - 2_1$ A^-	626.6263	34	93±3	$(3.2\pm0.1) \times 10^{26}$
2010/10/30.644	CH_3OH	$13_0 - 12_0$ E	625.7495	34	16±3	$(6.4\pm1.3) \times 10^{26}$
2010/10/30.644	CH_3OH	$13_{-1} - 12_{-1}$ E	627.1705	34	17±3	$(4.8\pm0.8) \times 10^{26}$
C/2009 P1 (Garradd)						
2012/02/17.211	HF	$J(1–0)$	1232.4762	17	66±18[f]	$(2.0\pm0.5) \times 10^{25}$
2012/02/22.875	$H^{35}Cl$	$J(1–0)$	625.9188[d]	34	<8[e]	$< 1.29 \times 10^{25}$
2012/02/22.875	$H^{37}Cl$	$J(1–0)$	624.9778[d]	34	<9[e]	$< 1.45 \times 10^{25}$
2012/02/22.875	CH_3OH	$3_2 - 2_1$ A^-	626.6263	34	39±2	$(2.6\pm0.1) \times 10^{27}$
2012/02/22.875	CH_3OH	$13_0 - 12_0$ E	625.7495	34	4±2	$(3.8\pm1.9) \times 10^{27}$
2012/02/22.875	CH_3OH	$13_{-1} - 12_{-1}$ E	627.1705	34	10±2	$(6.1\pm1.4) \times 10^{27}$
2012/02/17.405	H_2O	$1_{11}–0_{00}$	1113.3430	19	6607±156	$(10.8\pm2.7) \times 10^{28}$[g]
2012/02/23.327	H_2O	$1_{11}–0_{00}$	1113.3430	19	6313±10	$(6.85\pm0.02) \times 10^{28}$
2012/02/23.105	H_2O	$2_{11}–2_{02}$	752.0331	28	2496±6	$(8.05\pm0.02) \times 10^{28}$
2012/02/23.327	$H_2{}^{18}O$	$1_{11}–0_{00}$	1101.6983	19	69±5	$(1.51\pm0.11) \times 10^{26}$

Notes. [a] Mean date. [b] Line area in main beam brightness temperature scale measured on WBS spectra, except for HF (HRS spectrum) and H_2O lines (median of WBS and HRS retrievals). Errors correspond to 1-σ statistical noise, and upper limits correspond to 3-σ. Calibration errors (at most 5%) are not included. [c] Assuming $T_{kin} = 60$ K for 103P/Hartley 2, and a variable temperature law for C/2009 P1 (Garradd) (see text). [d] Frequency of the main hyperfine component $F(5/2–3/2)$. [e] Weighted average of the 3 hyperfine components. [f] Line area measured in the HRS spectrum. The line area measured in the WBS spectrum is 51±11 mK, but the retrieval is somewhat baseline-dependent. [g] Determined by fitting the whole map; the error reflects the dispersion of the retrievals at different points in the map.

The HRS was used in the nominal-resolution mode (250 kHz spectral resolution).

All lines were observed in the two orthogonal horizontal and vertical polarizations, and all observations, except one (H_2O mapping), were performed in the Single-Point mode (Table 1). To cancel the background radiation, the observations of HCl and HF were carried out in the frequency-switching observing mode (FSW) with a frequency throw of 94.5 MHz. Dual beam-switching was used for Single-Point observations of water. The mapping observation of the 1_{11}–0_{00} water line at 1113 GHz undertaken on 17 February 2012 covers a field of view of $3' \times 3'$. The Half Power Beam Width (i.e., beam size) for each setting is given in Table 2.

Comet C/2009 P1 (Garradd) was tracked using the latest ephemeris available from the JPL Horizons system, and the estimated pointing error is less than 2–3$''$ r.m.s. On the other hand, it turned out that the ephemeris available for 103P/Hartley 2 at the time of uploading the comet positions to the spacecraft resulted in a pointing error of 10$''$, corresponding to 30% of the beam size at the frequency of the HCl lines (Table 2). This pointing offset is taken into account when determining the production rate from the line area (the model can compute expected line intensities for beams not centred on the nucleus).

The data were first processed with the HIPE software (Ott, 2010), to obtain calibrated level-2 data products, and then exported to CLASS[2]. Vertical and horizontal polarizations were averaged, weighted by the root mean square amplitude, in order to increase the signal-to noise ratio. The main beam brightness temperature scale was computed using a forward efficiency of 0.96, and a beam efficiency of 0.75, 0.75, 0.74, and 0.71, for bands 1b, 2b, 4b, and 5a, respectively. Spectra obtained after baseline removal are shown in Figs 1–3, and the H_2O map is plotted in Fig. 4.

The HCl lines were not detected in either comet, and the 3-σ upper limits for the line intensities, considering the three hyperfine components with statistical-weight ratios, are given in Table 2. A marginal detection is obtained for

[2] http://www.iram.fr/IRAMFR/GILDAS

HF in comet C/2009 P1 (Garradd) in both the WBS (4.6-σ for the line area) and HRS (3.6-σ) spectra (Table 2, Fig. 1). However, the WBS spectrum presents strong baseline ripples due to the use of the FSW mode, and the line area retrieved from the WBS spectrum depends on the baseline removal. Therefore we used the line area measured on the HRS spectrum for the determination of the HF production rate. The HF line appears to be somewhat blueshifted in the comet rest frame, by –0.36±0.15 km s^{-1} and –0.61±0.22 km s^{-1} in the WBS and HRS spectra, respectively.

The H_2O and $H_2^{18}O$ lines are detected with high signal-to-noise ratios (Figs 2 and 4).

Spectra acquired with the WBS cover a large (4 GHz) bandwidth. Three methanol lines were serendipitously detected in WBS spectra of comet 103P/Hartley 2 acquired with the HCl setting: the $3_2 - 2_1$ A^- line at 626.6263 GHz, and two higher energy lines ($13_0 - 12_0$ E and $13_{-1} - 12_{-1}$ E) at 625.7495 GHz and 627.1705 GHz, respectively (Fig. 3, Table 2). Frequencies of the A^- and E lines are from Herbst et al. (1984) and Xu et al. (2008), respectively. In comet C/2009 P1 (Garradd), the CH_3OH line at 626.626 GHz is well detected (Fig. 3), whereas the 625.749 GHz and 627.171 GHz lines are only marginally detected (Table 2).

3. Analysis

3.1. Excitation models

We developed an excitation model to convert HCl and HF line intensities into molecular production rates, similar to models developed by Biver (1997) (see also Biver et al., 1999) for other molecules. It computes the population distribution in the ground vibrational state $v = 0$, taking into account collisional excitation of the rotational levels by water molecules and electrons, infrared excitation of the $v = 1$ bands of vibration of HCl (at 2886 and 2883.9 cm^{-1} for $H^{35}Cl$ and $H^{37}Cl$, respectively) and HF (3961.4 cm^{-1}), and spontaneous decay. The v(1–0) band strengths are from Pine et al. (1985), and correspond to excitation rates (g-factors) at 1 AU from the Sun of 2.2×10^{-4} and 6.5×10^{-4} s^{-1} for HCl and HF, respectively (Crovisier, 2002). The rotational energy levels of the fundamental and excited bands are computed using the rotational constants provided by the JPL Molecular Spectroscopy database. Einstein-A and B coefficients of HCl and HF rotational transitions were computed using the dipole moments published by Kaiser (1970) and Muenter & Klemperer (1970), respectively.

The models used for analyzing the water and methanol lines consider the same excitation processes. For water lines, radiation trapping effects are important and considered in both excitation and radiative transfer calculations. Details on the H_2O and CH_3OH excitation models can be found in Bockelée-Morvan et al. (2012) and Biver et al. (2000), and references therein.

To model collisional excitation with water molecules (i.e., HCl–H_2O, HF–H_2O, CH_3OH–H_2O, and H_2O–H_2O collisions) we assume a total cross-section for de-excitation of the rotational levels of $\sigma_c = 5\times10^{-14}$ cm^2 (Bockelée-Morvan, 1987, and references therein). For comet 103P/Hartley 2, the gas kinetic temperature T_{kin} is taken equal to 60 K, corresponding to the rotational temperature of methanol lines (Sect. 3.4). Observations of comet C/2009 P1 (Garradd) are analyzed using the temperature law constrained by the observations of water (Sect. 3.2). Collisions by electrons are treated following, e.g., Zakharov et al. (2007), with the electron density scaling factor x_{n_e} taken equal to 0.2 (Biver et al., 2007; Hartogh et al., 2010). The local density of the molecules is described by the Haser model (Haser, 1957). We use the photodissociation rates at $r_h = 1$ AU for the quiet Sun published by Huebner et al. (1992) (β(HCl) = 7.2×10^{-6} s^{-1} and β(HF) = 4.3×10^{-7} s^{-1}). We assume an outflow velocity of 0.65 km s^{-1} for both comets, as derived from the width of the line profiles.

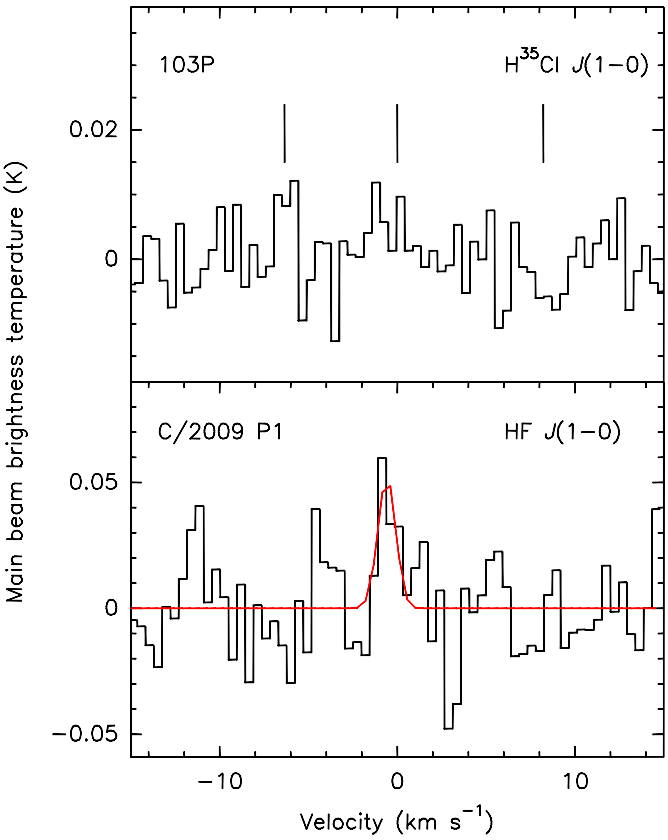

Fig. 1. Spectra of the $H^{35}Cl$ and HF J(1–0) lines observed in comets 103P/Hartley 2 and C/2009 P1 (Garradd) on 30 October 2010 and 17 February 2012, respectively, with the HRS. The HCl and HF spectra have been smoothed to a spectral resolution of 0.96 MHz (0.46 km s^{-1}) and 1.9 MHz (0.47 km s^{-1}), respectively. The position of the three $H^{35}Cl$ hyperfine components is indicated on the $H^{35}Cl$ spectrum. The red curve superimposed on the HF spectrum is a Gaussian fit to the line. The horizontal axis is the Doppler velocity based on the rest frequency of the transition.

3.2. Water in C/2009 P1 (Garradd)

Excitation conditions of the water molecule vary in the coma, and depend on the temperature radial profile. Therefore, the mapping observations of the 1_{11}-0_{00} line at 1113 GHz and the multiple-line observations of water can be used to constrain the excitation in the coma of comet C/2009 P1 (Garradd). Following the method outlined by Bockelée-Morvan et al. (2012), we obtain a better

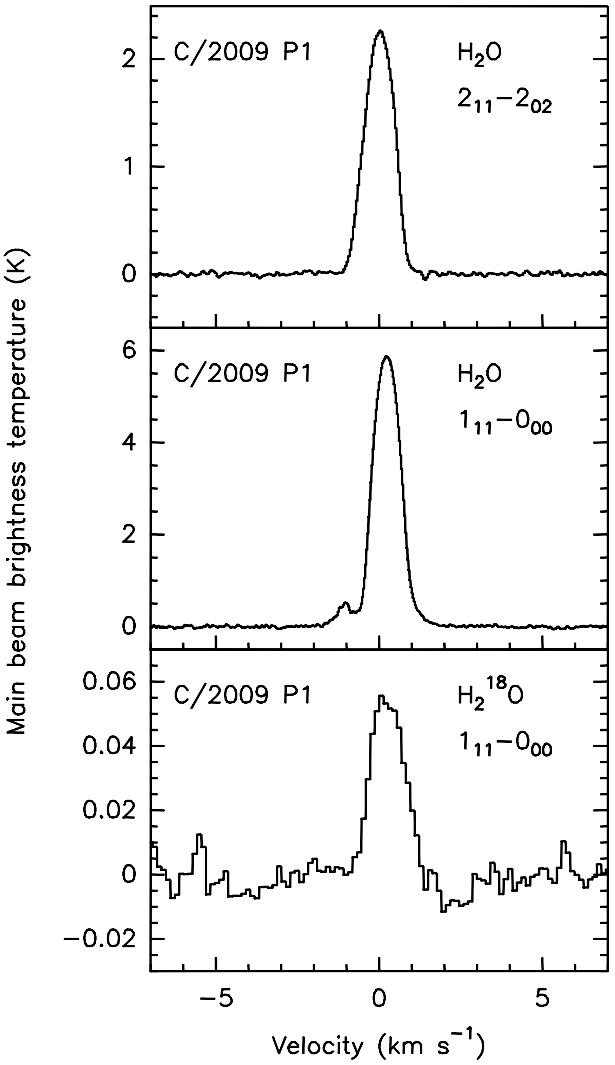

Fig. 2. H_2O and $H_2{}^{18}O$ lines observed in comet C/2009 P1 (Garradd) on 22 February 2012. The channel spacing of the 1_{11}–0_{00} and 2_{11}–2_{02} H_2O HRS spectra is 120 kHz, corresponding to 0.033 and 0.048 km s^{-1}, respectively. The WBS spectrum of the 1_{11}–0_{00} $H_2{}^{18}O$ line has a spectral resolution of 1 MHz (0.27 km s^{-1}). The horizontal axis is the Doppler velocity based on the rest frequency of the transition.

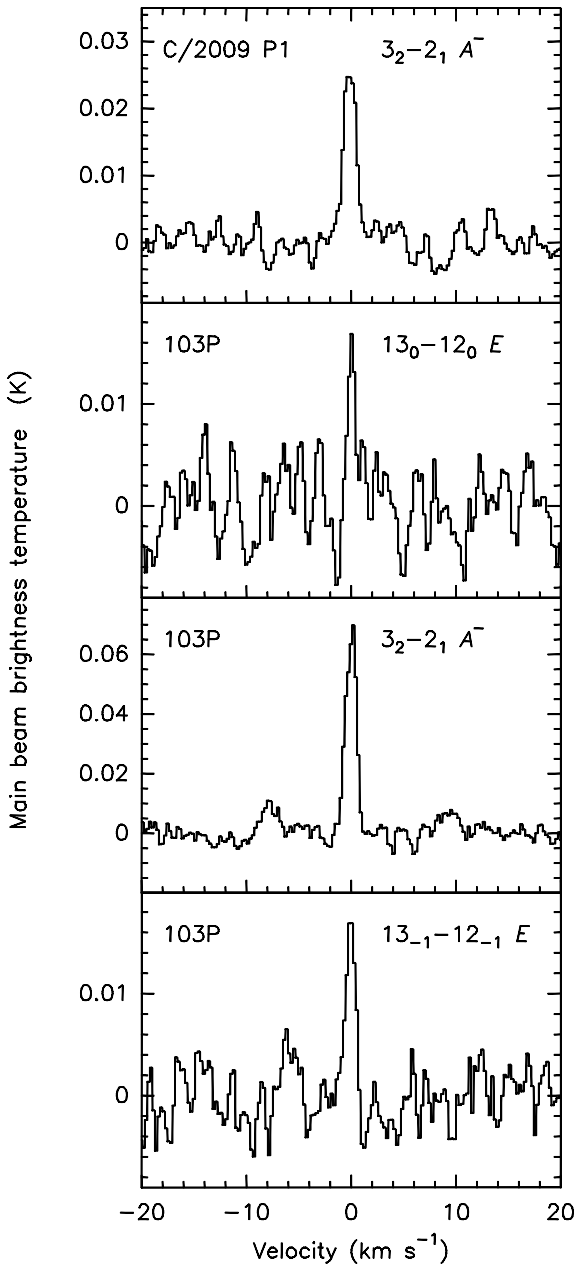

Fig. 3. CH_3OH lines observed in WBS spectra of comets 103P/Hartley 2 and C/2009 P1 (Garradd) observed on 30 October 2010 and 22 February 2012, respectively. The spectral resolution is 1 MHz (0.24 km s^{-1}). The horizontal axis is the Doppler velocity based on the rest frequency of the transition.

fit to the spatial evolution of the water line intensity using a temperature which varies with the distance to the nucleus. A variable temperature also reduces the difference between the production rates inferred from the 1113 GHz and 752 GHz lines observed on 23 February. In addition, based on the mean $Q(H_2O)$ deduced from the 1113 and 752 GHz H_2O lines, the inferred $Q(H_2^{16}O)/Q(H_2^{18}O)$ production rate ratio is then also closer to the value determined in the same comet in October 2011 (Bockelée-Morvan et al., 2012) and to the $^{16}O/^{18}O = 500$ Earth value. Indeed, we derive $Q(H_2^{16}O)/Q(H_2^{18}O) = 497 \pm 36$ using the variable temperature profile, whereas the value inferred using a constant temperature is lower (e.g., 429 ± 32 for $T_{kin} = 50$ K). This temperature profile has a minimum at 2500–10 000 km, with T_{kin} decreasing from 150 K to 20 K in the first 2500 km above the surface and increasing from 20 K at 10 000 km to 150 K at 20 000 km.

The measured water production rate for comet C/2009 P1 (Garradd) is then (1.1±0.3) × 10^{29} s^{-1} and (0.75±0.05) × 10^{29} s^{-1} for 17 and 23 February, respectively, where the former value is determined by fitting the whole map, and the latter value is deduced from the $Q(H_2{}^{18}O)$ value, assuming the terrestrial $^{16}O/^{18}O = 500$ ratio (Table 2). These post-perihelion $Q(H_2O)$ measurements, taken 60 days after perihelion, are about two times lower than the *Herschel* determination obtained 80 days before perihelion (Bockelée-Morvan et al., 2012). They are are in good agreement with values of $\sim 1 \times 10^{29}$ s^{-1} derived for 17 and 20 February 2012 from Ly-α measurements using

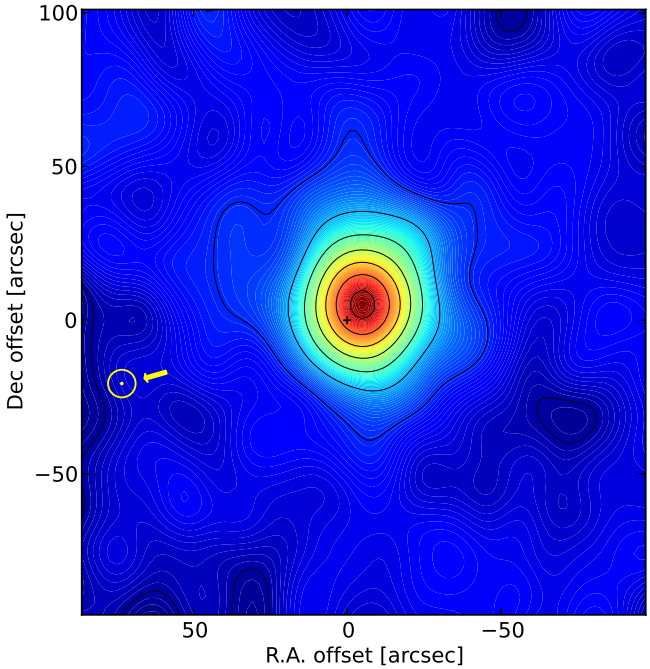

Fig. 4. On-the-fly map of the 1_{11}–1_{00} para H_2O line at 1113 GHz in comet C/2009 P1 (Garradd) obtained with the WBS on 17 February 2012. The contour spacing is 0.6 K km s^{-1} in main beam brightness temperature scale. The cross is at (0,0) coordinates. The Sun direction is indicated by the arrow. The beam size is 19″.

the Solar Wind ANisotropy (SWAN) instrument onboard the Solar Heliospheric Observatory (SOHO) (Combi et al., 2013), and with the OH production rate of (1.12±0.08) × 10^{29} s^{-1} measured with the Nançay radio telescope (average of 13–25 February) (Crovisier et al., in preparation).

The water map shown in Fig. 4 shows excess emission towards North-West, approximately in the tail direction (at PA = 286°). The offset between the position of the peak and the nucleus position obtained from the JPL Horizons ephemeris is about 6.5″ NW in the WBS and HRS maps. A similar offset of the brightness peak in the approximately anti-solar direction is also present in the pre-perihelion water maps taken with *Herschel* (Bockelée-Morvan et al., 2012). This excess emission in the anti-sunward quadrant resembles that observed for comet 103P/Hartley 2 (Meech et al., 2011; Knight & Schleicher, 2013) and can be explained by water production from an icy grain halo accelerated in the tail direction. Other indications that sublimating icy grains were present around C/2009 P1 (Garradd) are presented by Paganini et al. (2012), Combi et al. (2013), and DiSanti et al. (2014). The asymmetric shape of the activity curve and larger production rate before perihelion is interpreted by Combi et al. (2013) as the result of the presence of a substantial amount of sublimating icy grains/chunks pre-perihelion, possibly combined with seasonal effects. The water maps obtained with *Herschel* suggest a contribution from icy grains both pre and post-perihelion.

3.3. HCl and HF

The derived production rates (3-σ upper limits for $H^{35}Cl$ and $H^{37}Cl$) are given in Table 2. The terrestrial ^{35}Cl and ^{37}Cl abundances are of 75.77% and 24.23% chlorine atoms, respectively (Rosman & Taylor, 1998). This isotopic ratio is used to determine 3-σ upper limits for the HCl production rate from the $Q(H^{35}Cl)$ and $Q(H^{37}Cl)$ values. We infer $Q(HCl) < 1.34 \times 10^{24}$ s^{-1} and $Q(HCl) < 1.60 \times 10^{25}$ s^{-1}, for comets 103P/Hartley 2 and C/2009 P1 (Garradd), respectively.

In Table 3, production rate measurements have been normalized to the water production rate to constrain the HCl and HF content in cometary ices. Numerous measurements of the water production rate have been obtained for 103P/Hartley 2 near the time of EPOXI closest approach on 4 November 2010, including using *Herschel* (Lis et al., 2010; Biver et al., 2011; Dello Russo et al., 2011; Combi et al., 2011; Crovisier et al., 2013; Hartogh et al., 2011; Mumma et al., 2011; Meech et al., 2011). Comet 103P/Hartley 2 displayed large, rotation-induced, gas-activity variations, so we used contemporaneous H_2O data for the normalization. We assumed the value $Q(H_2O) = 1.2 \times 10^{28}$ s^{-1}, deduced from *Herschel* H_2O observations performed on 30.607 and 30.623 October, i.e., just before the HCl observations (Lis et al., 2010, N. Biver, personal communication). This value is consistent with the value deduced from *Odin* observations of the H_2O 557 GHz line obtained at the same time as the HCl observations (Biver et al., 2011).

The derived $Q(HCl)/Q(H_2O)$ 3-σ upper limits are 1.1 × 10^{-4} and 2.2 × 10^{-4} for 103P/Hartley 2 and C/2009 P1 (Garradd), respectively. Hence, a more sensitive upper limit for the HCl content in cometary ices is derived from the observations of 103P/Hartley 2. For HF, we derive $Q(HF)/Q(H_2O) = (1.8\pm0.5) \times 10^{-4}$ in C/2009 P1 (Garradd), under the assumption that the marginal detected line is real. Using instead the r.m.s. of the HRS spectrum, we derive $Q(HF)/Q(H_2O) < 1.5 \times 10^{-4}$ (3-σ).

3.4. Methanol in 103P/Hartley 2 and C/2009 P1 (Garradd)

The intensities of the three observed methanol lines allow us to determine the rotational temperature of methanol. For comet C/2009 P1 (Garradd), the high-energy $13_0 - 12_0$ E (625.749 GHz) and $13_{-1} - 12_{-1}$ E (627.171 GHz) lines are only marginally detected (Table 2). Since the upper levels of the transitions have similar energy and Einstein-A coefficient, we used their combined intensity (7 ± 1.6 mK km/s) to derive a rotational temperature of methanol of T_{rot} = 57±5 K. For comet 103P/Hartley 2, the three lines are well detected and we infer T_{rot} = 60±3 K.

Methanol production rates are given in Table 2. For 103P/Hartley 2, the mean production rate, averaging values from the three lines is $Q(CH_3OH) = (3.2\pm0.4) \times 10^{26}$ s^{-1}, which is consistent with values published by Boissier et al. (2014) for 28 October 2010, keeping in mind that the gaseous activity of comet 103P/Hartley 2 was strongly variable (A'Hearn et al., 2011; Drahus et al., 2012). For comet C/2009 P1 (Garradd), we infer a weighted-mean value of $Q(CH_3OH) = (2.6\pm0.4) \times 10^{27}$ s^{-1}, similar to the value measured a week earlier with the 30-m telescope of the Institut de radioastronomie millimétrique (IRAM) (Biver et al., 2012). This corresponds to abundances rela-

Table 3. HCl and HF abundances and depletions with respect to solar cosmic abundances.

HX	Comet	$Q(\mathrm{HX})/Q(\mathrm{H_2O})^a$ ($\times 10^{-4}$)	$(\mathrm{X/O})_\odot{}^b$ ($\times 10^{-4}$)	Depletion factor
HCl	103P	$< 1.1^c$	$6.5^{+6.4}_{-3.2}$	$> 6^{+6}_{-3}$
HCl	C/2009 P1	$< 2.2^d$	$6.5^{+6.4}_{-3.2}$	$> 3^{+3}_{-1}$
HF	C/2009 P1	1.8 ± 0.5^e	$0.74^{+0.74}_{-0.37}$	$0.4^{+0.4}_{-0.2}$

Notes. [a] Production rate ratio. [b] Solar abundances from Asplund et al. (2009), see text. [c] $Q(\mathrm{H_2O}) = 1.2 \times 10^{28}$ s^{-1}. [d] $Q(\mathrm{H_2O}) = 0.75 \times 10^{29}$ s^{-1}. [e] $Q(\mathrm{H_2O}) = 1.1 \times 10^{29}$ s^{-1}.

tive to water of 2.7±0.3 % and 3.4 ± 0.6 %, for comets 103P/Hartley 2 and C/2009 P1 (Garradd), respectively, assuming water production rates of 1.2×10^{28} and 0.75×10^{28} s^{-1}, respectively (see Sects 3.2 and 3.3).

4. Discussion

The F and Cl primordial Solar System abundances, that can be measured in the Sun, are uncertain. The solar photospheric values have been estimated to $(\mathrm{F/O})_\odot = 7.4^{+7.4}_{-3.7} \times 10^{-5}$ and $(\mathrm{Cl/O})_\odot = 6.5^{+6.4}_{-3.2} \times 10^{-4}$ (Asplund et al., 2009). However, the Cl/H value has been measured precisely in nearby HII regions, and suggests $(\mathrm{Cl/O})_\odot = (4.27\pm 0.9) \times 10^{-4}$ (García-Rojas & Esteban, 2007). The abundance of chlorine has also been measured in solar flares from X-ray spectra of Cl XVI lines, from which $(\mathrm{Cl/O}) = 11.5^{+9.3}_{-5.2} \times 10^{-4}$ can be deduced. This high value could be representative of $(\mathrm{Cl/O})_\odot$, unless some fractionation processes separating ions and neutrals are occurring in the solar atmosphere (Sylwester et al., 2011).

Using the solar abundances from Asplund et al. (2009), the $Q(\mathrm{HCl})/Q(\mathrm{H_2O})$ production rate ratio measured for 103P/Hartley 2 is a factor of at least 3 to 12 lower than the primordial Solar System (Cl/O) abundance (Table 3). A depletion factor larger than 2–6 is obtained for comet C/2009 P1 (Garradd) (Table 3). On the other hand, the $Q(\mathrm{HF})/Q(\mathrm{H_2O})$ production rate ratio would be approximately consistent with the cosmic (F/O), taking into account error bars in $(\mathrm{F/O})_\odot$ (Table 3). The only other upper limit obtained for a halogen-bearing species in comets is for NaCl in comet C/1995 O1 (Hale-Bopp), which value is 8 $\times 10^{-4}$, i.e., a factor of 8 higher than the $Q(\mathrm{HCl})/Q(\mathrm{H_2O})$ upper limit measured in comet 103P/Hartley (Lis et al., 1997; Crovisier et al., 2004). It is important to note that we use the HCl and HF abundances relative to water as an indicator of the Cl/O and F/O abundances in cometary ices. However, other oxygen-bearing species are present in significant abundances, such as CO_2, CO, and CH_3OH. We therefore likely overestimate the Cl/O and F/O abundances in cometary ices by some factor when using the abundances relative to water. This factor is difficult to evaluate as the CO/H_2O and CO_2/H_2O relative abundances inside the nuclei are not precisely known. Comet 103P/Hartley 2 is CO–poor (Weaver et al., 2011) and CO_2–rich (A'Hearn et al., 2011), with a $Q(CO_2)/Q(H_2O)$ production rate ratio from the surface of 0.6, and most of the H_2O production coming from grains (Fougere et al., 2013). Comet C/2009 P1 (Garradd) has a typical CO_2/H_2O production rate ratio of 8% (Feaga et al., 2013) and is CO–rich, with $Q(\mathrm{CO})/Q(\mathrm{H_2O})$ varying from $\sim$ 10% to 60% along its orbit (Biver et al., 2012; Paganini et al., 2012; McKay et al., 2012; Feaga et al., 2013). Overall, we may overestimate the Cl/O and F/O abundance upper limits in cometary ices by 30–50%.

The Cl and F elemental abundances in the rocky phase of cometary nuclei are not known. Ishii et al. (2008) found chlorine in one Stardust impact track and one terminal particle, but determining the Cl elemental abundance would require averaging many particles. Cometary dust presents analogies with primitive carbonaceous chondrites. In the less differentiated CI meteorites, the Cl/Si and F/Si abundances, which are measured with high precision, are in the low range of estimated solar photospheric values (Asplund et al., 2009). Should these abundances be representative of the primordial Solar System abundances, then the depletion factor of Cl in cometary ices is > 3. On the other hand, the cometary F/O, suggested from the marginal HF detection, is higher than the cosmic value.

In the dense interstellar medium, where conditions may be representative of the presolar cloud, HCl and HF are found to be strongly depleted in the gas phase with respect to solar abundances. Since chemical models predict that HF and HCl are formed in important quantities in the gas phase, taking up to 100% of fluorine and several 10's of percent of chlorine (Schilke et al., 1995; Neufeld & Wolfire, 2009), it has been suggested that these species could be locked onto grains (Schilke et al., 1995; Peng et al., 2010; Emprechtinger et al., 2012). However, in the L1157-B1 shock, where species from volatile and refractory grain components are enhanced, the HCl abundance is surprisingly low, from which one proposed interpretation is that HCl is not the main reservoir of chlorine in the gas and icy phase of star-forming regions (Codella et al., 2012). HCl is also detected in the warm (250 K) compact circumstellar envelope or disk of CRL 2136, with a fractional abundance consistent with the expected HCl abundance at this temperature, and which corresponds to approximately 20% of the elemental chlorine abundance (Goto et al., 2013).

For the early solar nebula, thermodynamic calculations show that HCl gas is stable at high temperatures, NaCl becomes the dominant species at 1100 K, and Cl is sequestered in solid phase sodalite ($Na_8Al_6Si_6O_{24}Cl_2$) between 900 and 950 K (Fegley & Lewis, 1980). Chlorine will condense as solid HCl hydrates ($HCl \cdot 3H_2O$) when temperatures fall below 160 K (Zolotov & Mironenko, 2007). Pure HCl ice will condense at $\sim$ 50 K. Alternatively, reaction kinetics may be too slow, and Cl existed mainly as HCl gas in the solar nebula. This scenario is advocated by Zolotov & Mironenko (2007), who argue that the positive correlation between the Cl content in chondrites and the degree of aqueous alteration is more consistent with a delivery of chlorine as a component of water ice. This is also supported by the abundance of the short-lived radionuclide ^{36}Cl in calcium-aluminium-rich inclusions (Jacobsen et al., 2011). On the other hand, Sharp & Draper (2013) and Sharp et al. (2013) exclude this scenario on the basis of the ^{37}Cl/^{35}Cl isotopic ratio measured in chondrites. Interestingly, chlorine, as well as other halogens, are depleted on Earth by a factor of 10 relative to solar and chondritic abundances (possible interpretations for this deficiency are discussed in Sharp et al., 2013).

Comets likely formed in the early Solar System farther away than asteroids in the Main Belt, though plan-

etary migration resulted in a general shake-up of the small-body populations (Gomes et al., 2005; Walsh et al., 2011). Their ices are believed to be constituted of different phases, some molecules being direct tracers of interstellar chemistry, while others, including complex molecules, could have been formed in the protoplanetary disk (Hincelin et al., 2013). The observed depletion of HCl with respect to the solar $(Cl/O)_\odot$ abundance in cometary ices is consistent with HCl not being the main reservoir of chlorine in the regions of the solar nebula where comets formed, a result which is consistent with the observed depletion in the L1157-B1 shock (Codella et al., 2012). The observed depletion should provide constraints for models examining the chlorine chemistry in protoplanetary disks and in the solar nebula.

The HF/H_2O value derived in C/2009 P1 (Garradd) is consistent with the $(F/O)_\odot$ solar photospheric abundance, taking into account uncertainties in $(F/O)_\odot$, which would suggest that HF is the main fluorine compound in the gas phase of the outer solar nebula. However, it is a factor of three higher than the (F/O) solar value of 5.4×10^{-4} derived from the elemental composition of primitive CI meteorites. If this value is indeed representative of the fluorine Solar System abundance, then our marginal detection implies a large overabundance of fluorine in cometary ices, and therefore is probably not real. Hopefully, better constraints on the halogen content in cometary material will be obtained from the Rosetta mission (Glassmeier et al., 2007).

Acknowledgements. HIFI has been designed and built by a consortium of institutes and university departments from across Europe, Canada and the United States (NASA) under the leadership of SRON, Netherlands Institute for Space Research, Groningen, The Netherlands, and with major contributions from Germany, France and the US. Consortium members are: Canada: CSA, U.Waterloo; France: CESR, LAB, LERMA, IRAM; Germany: KOSMA, MPIfR, MPS; Ireland, NUI Maynooth; Italy: ASI, IFSI-INAF, Osservatorio Astrofisico di Arcetri-INAF; Netherlands: SRON, TUD; Poland: CAMK, CBK; Spain: Observatorio Astronmico Nacional (IGN), Centro de Astrobiologa (CSIC-INTA). Sweden: Chalmers University of Technology - MC2, RSS & GARD; Onsala Space Observatory; Swedish National Space Board, Stockholm University - Stockholm Observatory; Switzerland: ETH Zurich, FHNW; USA: Caltech, JPL, NHSC.

Support for this work was provided by NASA through an award issued by JPL/Caltech. MdVB acknowledges partial support from grants NSF AST-1108686 and NASA NNX12AH91H. S.S. was supported by polish MNiSW funds (181/N-HSO/2008/0).

References

A'Hearn, M. F., Belton, M. J. S., Delamere, W. A., et al. 2011, Science, 332, 1396
Asplund, M., Grevesse, N., Sauval, A. J., & Scott, P. 2009, ARA&A, 47, 481
Biver, N. 1997, Ph.D. Thesis, University Paris 7
Biver, N., Bockelée-Morvan, D., Crovisier, J., et al. 1999, AJ, 118, 1850
Biver, N., Bockelée-Morvan, D., Crovisier, J., et al. 2000, AJ, 120, 1554
Biver, N., Bockelée-Morvan, D., Crovisier, J., et al. 2011, EPSC-DPS Joint Meeting 2011, 938
Biver, N., Bockelée-Morvan, D., Crovisier, J., et al. 2007, Planet. Space Sci., 55, 1058
Biver, N., Bockelée-Morvan, D., Lis, D. C., et al. 2012, LPI Contributions, 1667, 6330
Bockelée-Morvan, D. 1987, A&A, 181, 169
Bockelée-Morvan, D., Biver, N., Swinyard, B., et al. 2012, A&A, 544, L15
Boissier, J., Bockelée-Morvan, D., Biver, N., et al. 2014, Icarus, 228, 197
Cazzoli, G., & Puzzarini, C. 2004, J. Mol. Spect., 226, 161
Codella, C., Ceccarelli, C., Bottinelli, S., et al. 2012, ApJ, 744, 164
Combi, M. R., Bertaux, J.-L., Quémerais, E., Ferron, S., Mäkinen, J. T. T. 2011, ApJ, 734, L6
Combi, M. R., Mäkinen, J. T. T., Bertaux, J.-L., et al. 2013, Icarus, 225, 740
Crovisier, J. 2002, http://www.lesia.obspm.fr/perso/jacques-crovisier/basemol
Crovisier, J., Bockelée-Morvan, D., Colom, P., et al. 2004, A&A, 418, 1141
Crovisier, J., Colom, P., Biver, N., Bockelée-Morvan, D., & Boissier, J. 2013, Icarus, 222, 679
De Lucia, F. C., Helminger, P., & Gordy, W. 1971, Phys. Rev. A, 3, 1849
De Lucia, F. C., Helminger, P., Cook, R. L., & Gordy, W. 1972, Phys. Rev. A, 6, 1324
Dello Russo, N., Vervack, R. J., Jr., Lisse, C. M., et al. 2011, ApJ, 734, L8
DiSanti, M. A., Villanueva, G. L., Paganini, L., et al. 2014, Icarus, 228, 167
Drahus, M., Jewitt, D., Guilbert-Lepoutre, A., Waniak, W., & Sievers, A. 2012, ApJ, 756, 80
Emprechtinger, M., Monje, R. R., van der Tak, F. F. S., et al. 2012, ApJ, 756, 136
Feaga, L.M., A'Hearn, M.F., Farnham, T.L., et al. 2013, AJ, 147, 24
Fegley, B., Jr., & Lewis, J. S. 1980, Icarus, 41, 439
Fougere, N., Combi, M. R., Rubin, M., & Tenishev, V. 2013, Icarus, 225, 688
García-Rojas, J., & Esteban, C. 2007, ApJ, 670, 457
Glassmeier, K.-H., Boehnhardt, H., Koschny, D., Kührt, E., & Richter, I. 2007, Space Sci. Rev., 128, 1
Gomes, R., Levison, H. F., Tsiganis, K., & Morbidelli, A. 2005, Nature, 435, 466
Goto, M., Usuda, T., Geballe, T. R., et al. 2013, A&A558, L5
de Graauw, Th., Helmich, F.P., Phillips, T.G., et al. 2010, A&A, 518, L6
Hartogh, P., Lellouch, E., Crovisier, J. et al. 2009, P&SS, 57, 1596
Hartogh, P., Lis, D. C., Bockelée-Morvan, D., et al. 2011, Nature, 478, 218
Hartogh, P., Crovisier, J., de Val-Borro, M., et al. 2010, A&A, 518, L150
Haser, L. 1957, Bulletin de la Société Royale des Sciences de Liège, 43, 740
Herbst, E., Messer, J. K., de Lucia, F. C., & Helminger, P. 1984, J. Mol. Spect., 108, 42
Hincelin, U., Wakelam, V., Commerçon, B., Hersant, F., & Guilloteau, S. 2013, ApJ, 775, 44
Huebner, W. F., Keady, J. J., & Lyon, S. P. 1992, Ap&SS, 195, 1
Ishii, H. A., Brennan, S., Bradley, J. P., et al. 2008, Meteoritics and Planetary Science, 43, 215
Jacobsen, B., Matzel, J., Hutcheon, I. D., et al. 2011, ApJ, 731, L28
Johns, J. W. C. 1985, J. Opt. Soc. Am. B, 2, 1340
Kaiser, E. W. 1970, J. Chem. Phys., 53, 1686
Knight, M. M., & Schleicher, D. G. 2013, Icarus, 222, 691
Lis, D. C., Bockelee-Morvan, D., Biver, N., et al. 2010, IAU Circ., 9185, 2
Lis, D. C., Mehringer, D. M., Benford, D., et al. 1997, Earth Moon and Planets, 78, 13
McKay, A., Chanover, N., DiSanti, M., et al. 2012, AAS/Division for Planetary Sciences Meeting Abstracts, 44, #506.09
Meech, K. J., A'Hearn, M. F., Adams, J. A., et al. 2011, ApJ, 734, L1
Monje, R. R., Emprechtinger, M., Phillips, T. G., et al. 2011, ApJ, 734, L23
Monje, R. R., Lis, D. C., Roueff, E., et al. 2013, ApJ, 767, 81
Muenter, J. S., & Klemperer, W. 1970, J. Chem. Phys., 52, 6033
Mumma, M. J., Bonev, B. P., Villanueva, G. L., et al. 2011, ApJ, 734, L7
Neufeld, D. A., & Wolfire, M. G. 2009, ApJ, 706, 1594
Neufeld, D. A., Sonnentrucker, P., Phillips, T. G., et al. 2010, A&A, 518, L108
Nolt, I. G., Radostitz, J. V., Dilonardo, G., et al. 1987, J. Mol. Spect., 125, 274
Ott, S. 2010, ASP Conference Series, 434, 139
Paganini, L., Mumma, M. J., Villanueva, G. L., et al. 2012, ApJ, 748, L13
Pearson, J. C., 1995, Ph.D. Thesis, Duke University
Peng, R., Yoshida, H., Chamberlin, R. A., et al. 2010, ApJ, 723, 218

Pickett, H. M., Poynter, R. L., Cohen, E. A., et al. 1998, J. Quant. Spectrosc. Radiat. Transfer, 60, 883
Pilbratt, G. L., Riedinger, J. R., Passvogel, T., et al. 2010, A&A, 518, L1
Pine, A.S., Fried, A., Elkins, J.W. 1985, J. Mol. Spect., 109, 30
Rosman, K.J.R., & Taylor, P.D.P. 1998, J. Phys. Chem. Ref. Data, 27, 1275
Schilke, P., Phillips, T. G., & Wang, N. 1995, ApJ, 441, 334
Sharp, Z. D., & Draper, D. S. 2013, Earth and Planetary Science Letters, 369, 71
Sharp, Z. D., Mercer, J. A., Jones, R. H., et al. 2013, Geochim. Cosmochim. Acta, 107, 189
Sylwester, B., Phillips, K. J. H., Sylwester, J., & Kuznetsov, V. D. 2011, ApJ, 738, 49
Walsh, K. J., Morbidelli, A., Raymond, S. N., O'Brien, D. P., & Mandell, A. M. 2011, Nature, 475, 206
Weaver, H. A., Feldman, P. D., A'Hearn, M. F., Dello Russo, N., & Stern, S. A. 2011, ApJ, 734, L5
Xu, L.-H., Fisher, J., Lees, R. M., et al. 2008, J. Mol. Spect., 251, 305
Yu, S., Pearson, J. C., Drouin, B. J., et al. 2012, J. Mol. Spectrosc., 279, 16
Zakharov, V., Bockelée-Morvan, D., Biver, N., Crovisier, J., & Lecacheux, A. 2007, A&A, 473, 303
Zolotov, M. Y., & Mironenko, M. V. 2007, Lunar and Planetary Institute Science Conference Abstracts, 38, 2340